Article

Cell Reports

Functional Proteomics Identifies a PICS Complex Required for piRNA Maturation and Chromosome Segregation

Graphical Abstract

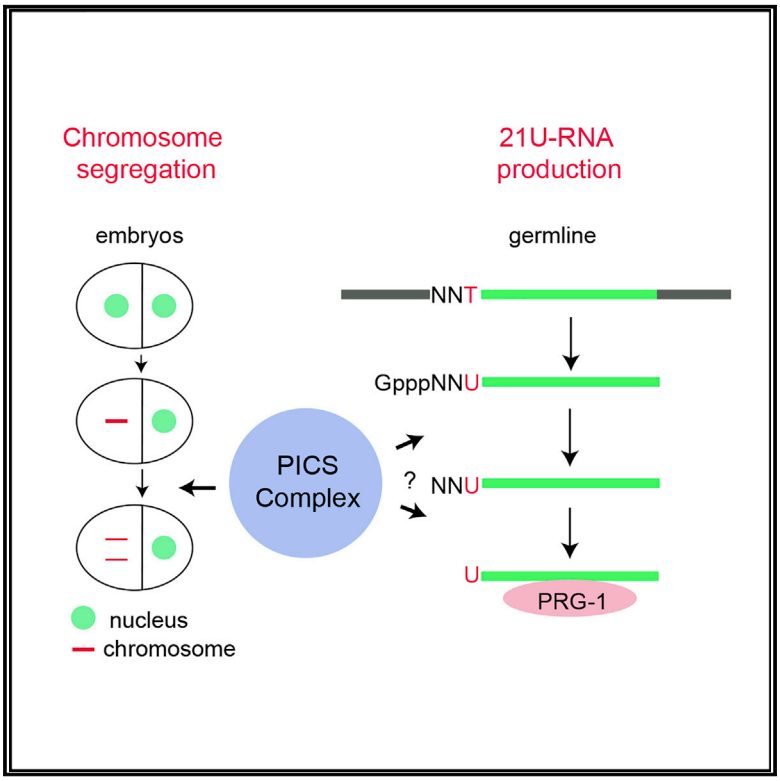

Authors

Chenming Zeng, Chenchun Weng, Xiaoyang Wang, ..., Xuezhu Feng, Chao Xu, Shouhong Guang

Correspondence

fengxz@ustc.edu.cn (X.F.), xuchaor@ustc.edu.cn (C.X.), sguang@ustc.edu.cn (S.G.)

In Brief

Zeng et al. use functional proteomics and identify a PICS complex that promotes Piwi-interacting RNA (piRNA) production in *C. elegans*. This work reports that the PICS complex acts in the 5′ end processing of piRNA precursors. This PICS complex also shuttles between the nucleus and cytoplasm and promotes chromosome segregation in embryos.

Highlights

- Functional proteomics identifies a PICS complex
- PICS complex is required for 21U-RNA maturation
- PICS complex promotes chromosome segregation
- The dual functions of PICS complex are independent of each other

Zeng et al., 2019, Cell Reports *27*, 3561–3572
June 18, 2019
https://doi.org/10.1016/j.celrep.2019.05.076

CellPress

Cell Reports
Article

Functional Proteomics Identifies a PICS Complex Required for piRNA Maturation and Chromosome Segregation

Chenming Zeng,[1,4] Chenchun Weng,[1,4] Xiaoyang Wang,[1,4] Yong-Hong Yan,[2,4] Wen-Jun Li,[2] Demin Xu,[1] Minjie Hong,[1] Shanhui Liao,[1] Meng-Qiu Dong,[2] Xuezhu Feng,[1,*] Chao Xu,[1,*] and Shouhong Guang[1,3,5,*]

[1]Hefei National Laboratory for Physical Sciences at the Microscale, School of Life Sciences, University of Science and Technology of China, Hefei, Anhui 230027, P.R. China

[2]National Institute of Biological Sciences, Beijing 102206, China

[3]CAS Center for Excellence in Molecular Cell Science, Chinese Academy of Sciences, Hefei, Anhui 230027, P.R. China

[4]These authors contributed equally

[5]Lead Contact

*Correspondence: fengxz@ustc.edu.cn (X.F.), xuchaor@ustc.edu.cn (C.X.), sguang@ustc.edu.cn (S.G.)

https://doi.org/10.1016/j.celrep.2019.05.076

SUMMARY

piRNAs play significant roles in suppressing transposons and nonself nucleic acids, maintaining genome integrity, and defending against viral infections. In *C. elegans*, piRNA precursors are transcribed in the nucleus and are subjected to a number of processing and maturation steps. The biogenesis of piRNAs is not fully understood. We use functional proteomics in *C. elegans* and identify a piRNA biogenesis and chromosome segregation (PICS) complex. The PICS complex contains TOFU-6, PID-1, PICS-1, TOST-1, and ERH-2, which exhibit dynamic localization among different subcellular compartments. In the germlines, the PICS complex contains TOFU-6/PICS-1/ERH-2/PID-1, is largely concentrated at the perinuclear granule zone, and engages in piRNA processing. During embryogenesis, the TOFU-6/PICS-1/ERH-2/TOST-1 complex accumulates in the nucleus and plays essential roles in chromosome segregation. The functions of these factors in mediating chromosome segregation are independent of piRNA production. We speculate that differential compositions of PICS factors may help cells coordinate distinct cellular processes.

INTRODUCTION

Piwi-interacting RNAs (piRNAs) are a class of small (21–30 bp) RNAs that are associated with Piwi, a member of the highly conserved Argonaute/Piwi protein family, and play significant roles in fertility and genome stability (reviewed by Watanabe and Lin, 2014; Weick and Miska, 2014). In *C. elegans*, piRNAs protect genome integrity in the germline by recognizing and silencing nonself sequences, such as transposons or other foreign nucleic acids, and they induce chromatin modification and neuron regeneration (Ashe et al., 2012; Bagijn et al., 2012; Feng and Guang, 2013; Kim et al., 2018; Luteijn and Ketting, 2013; Malone and Hannon, 2009; Mao et al., 2015; Shirayama et al., 2012).

In *C. elegans*, piRNA precursors are transcribed from thousands of genomic loci in the germline, mainly including two large genome clusters on chromosome IV (Gu et al., 2012; Weick et al., 2014). The upstream sequence transcription complex (USTC)—containing PRDE-1, SNPC-4, TOFU-4, and TOFU-5—has been identified to bind the Ruby motif and drive the transcription of piRNA precursors (Weng et al., 2019). Precursors are decapped at the 5′ ends to remove the first two nucleotides and trimmed at the 3′ ends to remove extra nucleotides and generate mature piRNAs (Billi et al., 2012; de Albuquerque et al., 2014; Gu et al., 2012; Tang et al., 2016). PARN-1, a conserved exonuclease present in germline P-granules, is required for 3′-end processing of piRNA precursors (Tang et al., 2016). Additionally, PID-1 and TOFU-1/2/6/7 have been found to be essential for 5′-end and 3′-end processing of piRNA precursors by forward and reverse genetic screens (de Albuquerque et al., 2014; Goh et al., 2014). Since most mature piRNAs are 21 nt in length and start with 5′-monophosphorylated uracil, piRNAs are also termed 21U-RNAs in *C. elegans* (Bagijn et al., 2012; Batista et al., 2008; Das et al., 2008; Gu et al., 2012; Ruby et al., 2006). The term 21U-RNA is used hereafter.

21U-RNAs scan for foreign sequences, while allowing mismatched pairing with targeted mRNAs (Ashe et al., 2012; Bagijn et al., 2012; Lee et al., 2012; Shen et al., 2018; Shirayama et al., 2012; Zhang et al., 2018). Upon targeting, the 21U-RNA/PRG-1 complex recruits RNA-dependent RNA polymerase (RdRP) to elicit the generation of secondary small interfering RNAs (siRNAs) to conduct subsequent gene-silencing processes (Ashe et al., 2012; Bagijn et al., 2012; Lee et al., 2012; Mao et al., 2015; Shirayama et al., 2012).

However, the mechanism by which 21U-RNA precursors are processed to generate mature 21U-RNAs remains elusive. Here, using functional proteomics, we identified a piRNA biogenesis and chromosome segregation (PICS) complex that is required for 21U-RNA maturation, faithful chromosome segregation, and cell division. The components of the PICS complex—TOFU-6, PICS-1, ERH-2, PID-1, and TOST-1—exhibit dynamic localization among different subcellular compartments. We

propose that differential compositions of PICS factors may help cells coordinate distinct cellular processes.

RESULTS

TOFU-6 Is Required for 21U-RNA Biogenesis, Chromosome Segregation, and Cell Division

A previous genome-wide RNAi screen identified seven Twenty-One-u Fouled Ups (TOFUs) that are engaged in distinct expression and processing steps of 21U-RNAs (Goh et al., 2014). Recently, we found that TOFU-4/5, PRDE-1, and SNPC-4 form a USTC to promote the transcription of 21U-RNA precursors (Weng et al., 2019). To further understand the biogenesis of 21U-RNAs, we constructed GFP-3xFLAG-tagged TOFU-1/2/6 transgenes (abbreviated as TOFU::GFPs) using Mos1-mediated single-copy insertion (MosSCI) technology (Frøkjaer-Jensen et al., 2008). Among the transgenes, TOFU-1/2s were expressed in the germline cytoplasm (Figure S1A). TOFU-6::GFP was present not only in the germline cytoplasm, but also at distinct perinuclear foci in the germline, and largely colocalized with the P-granule marker PGL-1 (Figures 1A and S1B). TOFU-6 did not form granules in oocytes and embryos, unlike PRG-1 and PGL-1 (Figures S1B and S1C) (Batista et al., 2008). The TOFU-6::GFP transgene reversed the sterile phenotype of *tofu-6*(*ust94*), suggesting that the transgene recapitulates the functions of the endogenous TOFU-6 protein (Figure S1D).

We focused on TOFU-6 and obtained two balanced mutants, *tofu-6(it20)* and *tofu-6*(*yt2*), from the Caenorhabditis Genetics Center (Figure 1B). To facilitate genotyping and genetic manipulation of *tofu-6*, we further generated two additional deletion alleles, *ust94* and *ust95*, by dual small guide RNA (sgRNA)-mediated CRISPR/Cas9 technology on a +/*mIn1* balanced background (Chen et al., 2014). *Ust94* caused a 107-amino-acid deletion and a frameshift, which likely results in a null allele. *Ust95* caused a 109-amino-acid in-frame deletion. We collected approximately 1000 homozygous *tofu-6* mutant worms of each allele and deep sequenced small RNAs 18–30 nt in size. 21U-RNAs were dramatically depleted in the *tofu-6* null mutants compared to wild-type worms (Figures 1C and S2A), which was consistent with previous results for *tofu-6* RNAi (Goh et al., 2014). We assayed type I and II 21U-RNAs and found that both classes of 21U-RNAs were depleted (Figure S2B). TOFU-6 was required for the expression of PRG-1. In *tofu-6* mutants, the expression level of GFP::PRG-1 was reduced (Figure S2C). T*ofu-6*(*ust94*) was used as the reference allele in this work.

We then assayed the brood sizes of *tofu-6* mutants. *Prg-1*, *pid-1*, *parn-1*, and *tofu-4* mutants all produced progeny, although these genes are essential for 21U-RNA production (Figure 1D) (de Albuquerque et al., 2014; Goh et al., 2014; Tang et al., 2016). Interestingly, the *it20*, *yt2*, and *ust94* alleles of *tofu-6* mutants were sterile, while the *tofu-6*(*ust95*) mutant still had a brood size similar to that of wild-type animals, suggesting that TOFU-6 has additional roles other than promoting 21U-RNA biogenesis and that *tofu-6*(*ust95*) is defective in some of these functions (Figure 1D).

The *tofu-6* mutant was previously reported with a maternal-effect lethal phenotype and was therefore named *mel-47* (Minasaki and Streit, 2007). We used GFP::H2B as a chromatin marker and observed a pronounced chromosome-lagging phenomenon in early embryos of *tofu-6*(*ust94*) mutants, but not in *tofu-6*(*ust95*) mutants, in early embryos (Figure 1E). Additionally, in meta-telophase, the two daughter nuclei of *tofu-6*(*ust94*) did not separate completely, adopting the shape of a raindrop with bridges between the two daughter cell nuclei (Figure 1F).

We conclude that TOFU-6s have essential roles in both promoting 21U-RNA biogenesis and chromosome segregation.

Identification of TOFU-6 Binding Proteins by Functional Proteomics

We searched for proteins that interact with TOFU-6. First, we used coimmunoprecipitation followed by mass spectrometry (IP-MS) to identify candidate proteins that interact with TOFU-6 (Table S1). Next, we examined whether the identified candidates were required for the subcellular localization of TOFU-6 by feeding worms bacteria that expressed double-stranded RNA (dsRNA) targeting these genes. The genes that were required for the perinuclear granule localization of TOFU-6 are listed in Figure 2A. Among them, PID-1, which functions to promote 21U-RNA processing, was identified (de Albuquerque et al., 2014). In addition, we identified three genes required for the perinuclear granule localization of TOFU-6. C35D10.13 was named TOST-1 for twenty-one u antagonist-1 (see below) (Rodrigues et al., 2018). F35G12.11 is a homolog of human ERH-2 (enhancer of rudimentary homolog-2). Y23H5A.3 was named PICS-1 (required for PICS-1; see below).

When *pid-1* and *pics-1* were depleted by RNAi, TOFU-6 failed to form perinuclear granules, but the P-granule marker PGL-1 remained intact (Figure 2B). We generated deletion alleles—*pid-1*(*ust64*), *erh-2*(*ust101/qC1*), *tost-1*(*ust102/qC1*), *and tost-1*(*ust103/qC1*)—by dual sgRNA-mediated CRISPR/Cas9 technology and obtained a balanced strain, *pics-1*(*tm2417/hT2*), from the National BioResource Project (NBRP) (Figure S3A). In *pid-1* and *pics-1* mutants, TOFU-6 failed to form perinuclear granules (Figure 2C). The depletion of several known 21U-RNA biogenesis factors, including t*ofu-1/2/4*, *prg-1*, and *parn-1,* did not prevent TOFU-6 from forming perinuclear foci (Figure 2C). Interestingly, in the *pid-1* mutant, the TOFU-6 foci disassembled in the meiotic region, while in the *pics-1* mutant, the TOFU-6 foci disassembled in both the mitotic and meiotic regions (Figure S3B). However, when *tost-1* and *erh-2* were depleted by RNAi, the TOFU-6::GFP foci became larger and brighter (Figure 2D). The protein levels of TOFU-6::GFP remained unchanged after RNAi of *tost-1* and *erh-2* (Figure 2E). In addition, depletion of *erh-2* and *tost-1* did not change GFP::PGL-1 foci (Figure S3C).

TOFU-6, PICS-1, and ERH-2 Are Required for 21U-RNA Maturation

To test whether these factors are required for 21U-RNA biogenesis, we collected homozygous mutants from balancers and quantified the 21U-RNA levels by quantitative RT-PCR. In *pid-1, pics-1*, and *erh-2* animals, but not in *tost-1* mutants, the levels of 21ur-1 and 21ur-5045 were significantly reduced compared to those in wild-type animals (Figure 3A). We deep sequenced small RNAs 18–30 nt in size from *pics-1*, *erh-2*,

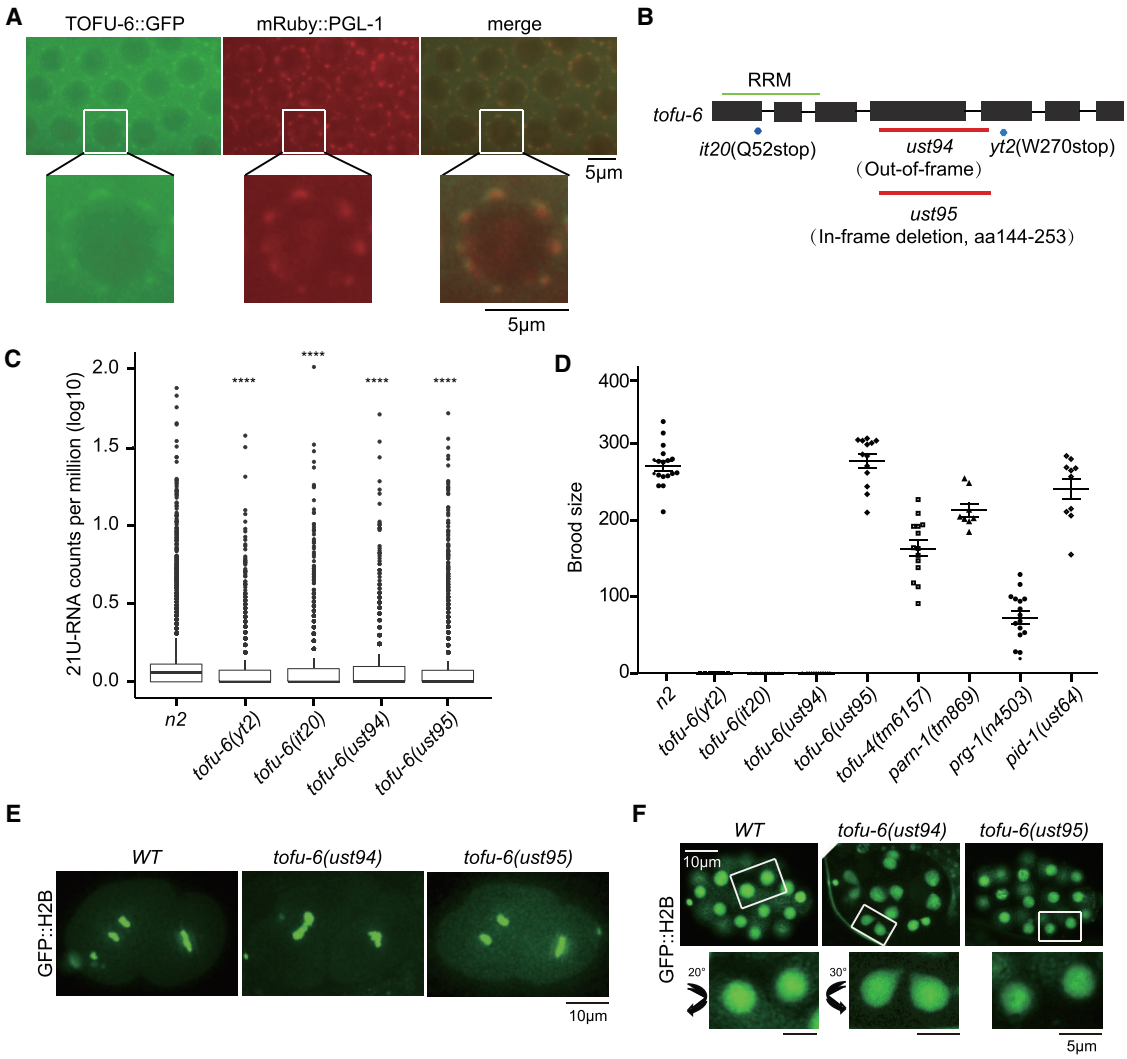

Figure 1. *Tofu-6* Is Required for 21U-RNA Biogenesis and Chromosome Segregation

(A) Images of TOFU-6::GFP and the P-granule marker mRuby::PGL-1 in germ cells.

(B) Schematic of the four alleles of *tofu-6*.

(C) Boxplots showing the normalized 21U-RNA reads in the indicated animals at the late young adult stage. The indicated mutant animals were isolated from balancers. Reads were normalized to total RNA reads. Significance tested with unpaired Wilcoxon test, ****$p < 2.2*e^{-16}$.

(D) Bar graph displaying the brood sizes of indicated worms. Worms were grown at 20°C, mean ± SD; ***$p < 0.001$, *$p < 0.05$, ns, not significant; n represents number of parental adults used, $n > 10$.

(E) Images of GFP::H2B at meta-anaphase in two-cell-stage embryos in indicated worms.

(F) Images of GFP::H2B in the indicated late-stage embryos.

tost-1, and *prg-1* mutants in the late young adult stage. Similar to *tofu-6* mutants, in *pics-1* and *erh-2* mutants, mature 21U-RNA levels were significantly reduced compared to those in wild-type animals (Figures 3B–3D). We assayed type I and II 21U-RNAs and found that both classes of 21U-RNAs were depleted in *pics-1* and *erh-2* mutants (Figure 3F). However, in *tost-1* mutants, we observed an increase in 21U-RNA levels, suggesting that TOST-1 might inhibit 21U-RNA accumulation (Figures 3A, 3B, and 3E). In addition, the presence of 21U-RNAs may be essential for the expression of PRG-1. In *tofu-6*, *pid-1*, *pics-1*, and *erh-2* mutants, but not in *tost-1* mutants, the expression of PRG-1 was significantly reduced compared to that in wild-type animals (Figures S2C, S4A, and S4B). We conclude that *tofu-6*, *pics-1*, and *erh-2* play essential roles in 21U-RNA biogenesis.

To understand the roles of PICS factors in 21U-RNA biogenesis, we treated small RNAs with the Tobacco Decapping Plus 2 (TDP2) enzyme to remove the 5′ end cap structure and then deep sequenced the RNA. 21U-RNA precursors mostly start 2 nt upstream of the 5′ end of mature 21U-RNAs and are capped with an m^7G (Gu et al., 2012). Removal of the 5′ end cap facilitates the sequencing of capped 21U-RNA precursors. We

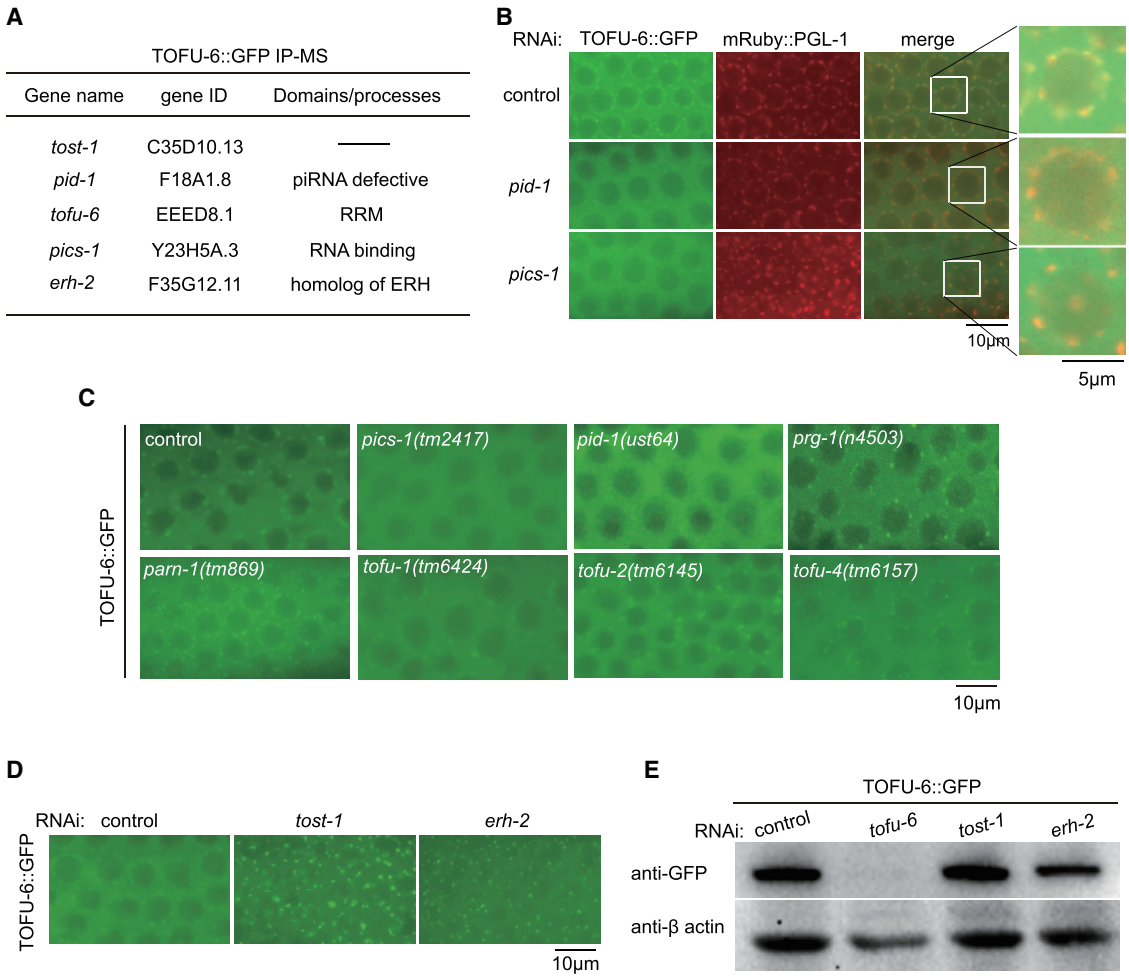

Figure 2. Identification of TOFU-6 Binding Proteins by Functional Proteomics

(A) Summary of IP-MS followed by feeding RNAi experiments for TOFU-6::GFP.

(B) Images of TOFU-6::GFP and the P-granule marker mRuby::PGL-1 after RNAi targeting of *pid-1* and *pics-1*.

(C) Images of TOFU-6::GFP in indicated animals.

(D) Images of TOFU-6::GFP after RNAi targeting of *tost-1 and erh-2*.

(E) Western blotting of TOFU-6::GFP after RNAi targeting of *tost-1* and *erh-2*.

analyzed the small RNA reads mapped to known *C. elegans* 21U-RNA loci with 2 nt upstream and 3 nt downstream, which included precursors, and likely other intermediates and degradation products with 1 or 2 nt upstream of the 5′ end and/or additional nucleotides downstream of the 3′ end, while the reads with sequences identical to mature 21U-RNA sequences were excluded. The reads with the 5′ cap were accumulated in *tofu-6*, *pics-1*, and *erh-2* mutants, compared to wild-type animals (Figure 4A). Then, we prepared small RNA libraries without decapping treatment by TDP2. Strikingly, although the reads including precursors and degradation products without the 5′ cap were rare, they increased in *tofu-6*, *pics-1*, and *erh-2* mutants, compared to wild-type animals (Figure 4B). We focused on the precursors starting at 2 nt upstream of the 5′ ends and found that they accumulated in *tofu-6*, *pics-1*, and *erh-2* mutants (Figures 4C and 4D). The length distribution of the precursors starting at 2 nt upstream of mature 21U-RNAs further supported the accumulation of precursors in the mutants (Figures S5A and S5B). The accumulation of precursors without the 5′ cap was exemplified by *21ur-22449* and *21ur-25884* (Figure S5C). In *prg-1* mutants, the 21U-RNA precursors without the 5′ cap were not increased, compared with those in wild-type animals (Figures 4B, 4D, and S5B). In addition, we noticed a higher coverage of 21U-RNA precursors starting at −1 nt than at −2 nt upstream of mature 21U-RNA sequences in the samples without TDP2 treatment (Figure 4B), which implied that the precursors were likely trimmed or degraded from −2 to −1 and then to position 0.

These data together suggest that TOFU-6, PICS-1, and ERH-2 function upstream of PRG-1 binding to 21U-RNA. Whether these factors are able to decap 21U-RNA precursors or trim extra nucleotides at 5′ ends needs further investigation (Figure 4E).

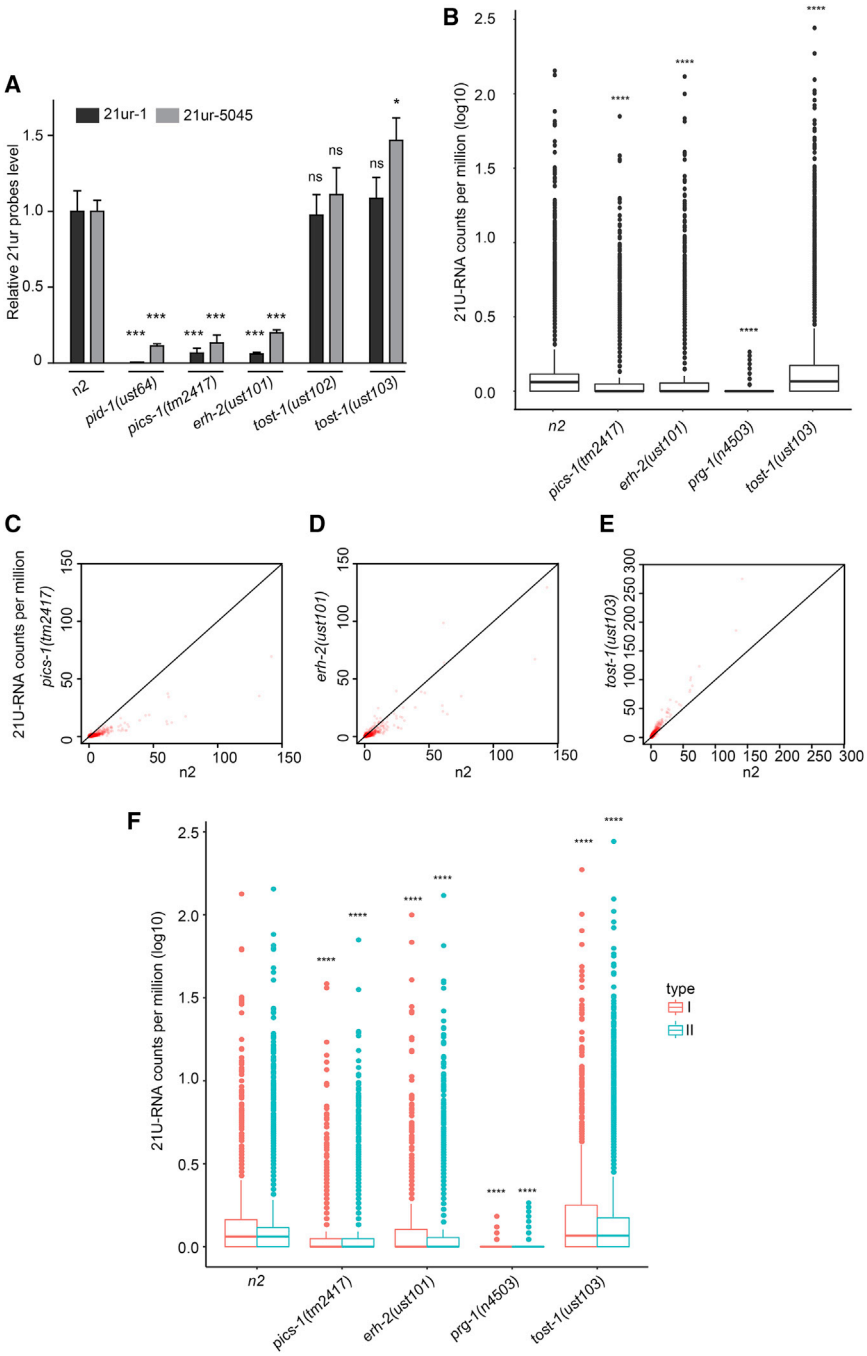

Figure 3. PICS-1 and ERH-2, but Not TOST-1, Are Required for 21U-RNA Biogenesis

(A) 21U-RNA levels detected by quantitative RT-PCR. Mean ± SD; ***p < 0.001, *p < 0.05; ns, not significant; n = 4 replicates.

(B) Boxplots displaying 21U-RNA counts per million (log10) in indicated animals at the late young adult stage. *Pics-1*, *erh-2*, *and tost-1* mutant animals were isolated from balancers. 21U-RNA reads were normalized to total mapped RNA reads. Significance was tested with unpaired Wilcoxon tests, ****p < $2.2*e^{-16}$.

(C–E) Scatterplots comparing the numbers of 21U-RNA reads between wild-type and *pics-1* (C), *erh-2* (D), and *tost-1* (E) mutant worms.

(F) Boxplots displaying type-I and type-II 21U-RNA counts per million (log10) in the indicated animals. Significance was tested with unpaired Wilcoxon tests, ****p < $2.2*e^{-16}$.

Subcellular Localization of PICS-1, ERH-2, PID-1, and TOST-1 in Germlines

We then constructed single-copy GFP::3xFLAG tagged PICS-1, PID-1, and TOST-1 transgenes by MosSCI and constructed GFP::3xFLAG tagged ERH-2 *in situ* with CRISPR knockin technologies. The transgenes reversed the sterile phenotypes of their respective mutants (Figure S6A). The expression patterns of PICS-1 and ERH-2 were similar to that of TOFU-6, which accumulated in both germline cytoplasm and perinuclear nuage and largely overlapped with the P-granule marker PGL-1 (Figures 5A, 5B, S6B, and S6C). PID-1 mainly accumulated in perinuclear nuage, and TOST-1 mainly accumulated in the cytosol of the germline syncytium but did not significantly accumulate in the perinuclear granules (Figures 5C, 5D, S6D, and S6E).

Similar to the case for TOFU-6 granules after the depletion of *tost-1* and *erh-2*, RNAi knock down of *tost-1* and *erh-2* induced larger and brighter PICS-1 granules (Figures S7A and S7B), and RNAi knock down of *tost-1* induced larger and brighter ERH-2 granules (Figures S7C and S7D). In *pid-1* mutants, the PICS-1 foci disassembled in the meiotic region, while the ERH-2 foci disassembled in both the mitotic and meiotic regions (Figures S7E and S7F). Strikingly, PICS-1::GFP and PID-1::GFP failed to form peri-nuclear granules but accumulated in the nucleus upon *tofu-6* RNAi, and ERH2::GFP failed to form perinuclear granules but accumulated in the nucleus upon *pics-1* and *tofu-6* RNAi, suggesting that PICS-1, PID-1, and ERH-2 may shuttle between the cytoplasm and the nucleus in the germline (Figures S7G–S7I). Interestingly, the expression levels of TOST-1 were strongly reduced in the germline and in embryos upon the depletion of *pics-1* and *erh-2* (Figure S7J; see also Figures 7D and S10C).

Since P granules and PICS granules largely overlapped with each other in the perinuclear region in the germline cells, we investigated the relationship between these two types of granules. Depletion of PICS genes only affected the formation of PICS granules, but not the formation of P granules, as indicated by the marker PGL-1 (Figures 2B and S3C). Similarly, RNAi

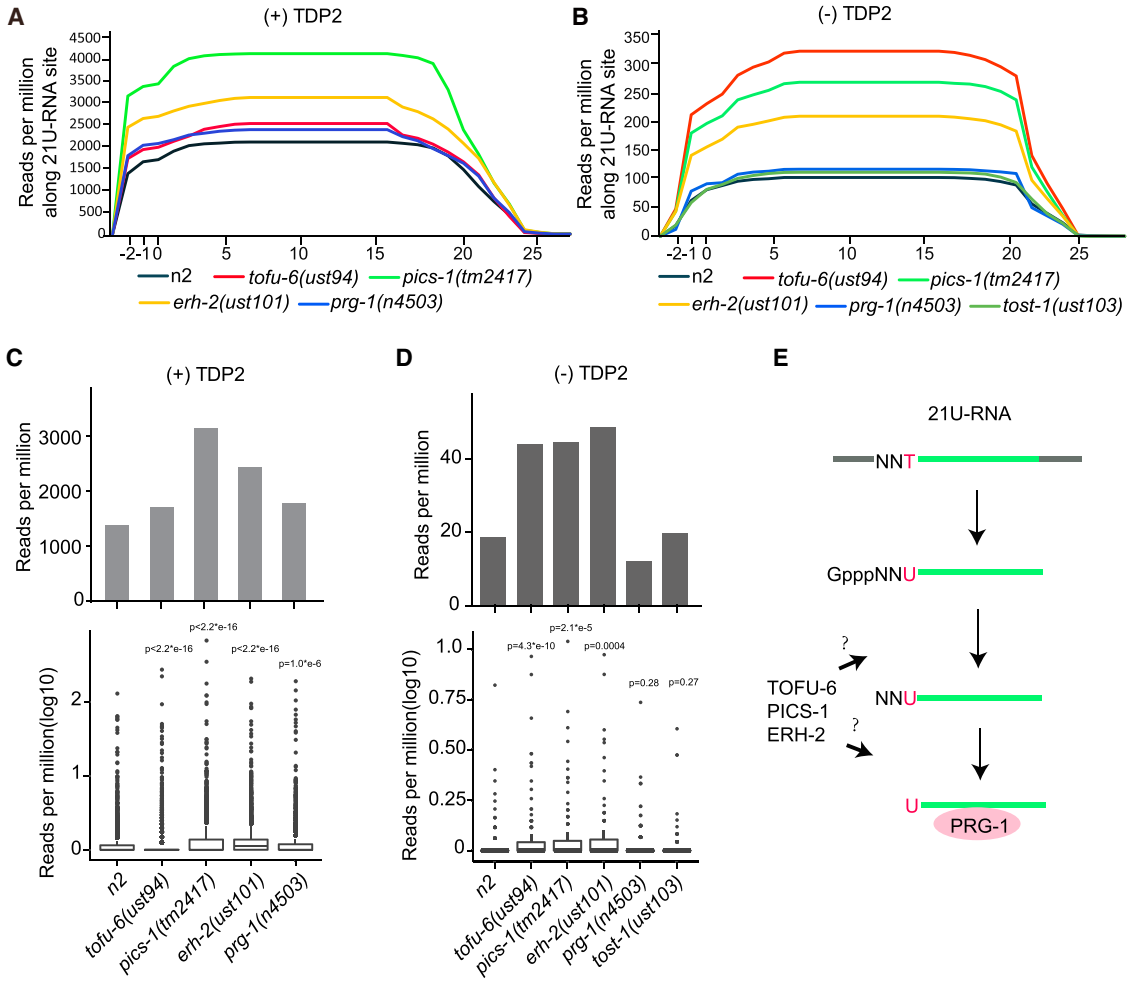

Figure 4. 21U-RNA Precursors Accumulate in *tofu-6*, *pics-1*, and *erh-2* Animals

(A and B) Number of small RNA reads that mapped to 21U-RNA loci with 2 nt upstream and 3 nt downstream, which included precursors and likely other intermediates and degradation products with 1 nt or 2 nt upstream of 5′ ends and/or additional nucleotides downstream of 3′ ends with (A) or without (B) decapping treatment, while the reads with sequences identical to mature 21U-RNA sequences were excluded. The annotated 5′ ends of the 21U-RNAs are at position 0. Reads were normalized to total mapped small RNA reads.

(C and D) Number of 21U-RNA precursors starting at 2 nt upstream of 5′ ends of 21U-RNAs with (C) or without (D) decapping treatment in mutants and wild-type animals. Bar plot displaying total precursors (top panel) and boxplots displaying individual precursors (bottom panel). Reads were normalized to total mapped small RNA reads. Significance was tested with unpaired Wilcoxon tests, and p values were indicated in the graphs.

(E) A diagram displaying the biogenesis of 21U-RNAs.

knock down of *csr-1* and *glh-1*, two P-granule components, failed to disrupt the PICS foci (Figure 5E). Although the localization of many P-granule components is not disrupted by *csr-1* or *glh-1* RNAi, these results raise the possibility that P granules and PICS granules are distinct from each other.

TOFU-6, PICS-1, ERH-2, PID-1, and TOST-1 Form Protein Complexes

To further test whether these factors form a protein complex, we first assayed the protein-protein interactions of these proteins *in vitro*. HA-His- or GST-tagged TOFU-6, PICS-1, ERH-2, PID-1, and TOST-1 proteins were expressed in *E. coli* and purified. Then, the proteins were mixed together and pulled down by GST beads. After extensive elution, the associated proteins were eluted and detected by western blotting with anti-HA antibodies (Figures 6A–6D). Next, we investigated the *in vivo* protein-protein interactions by immunoprecipitating 3xFLAG-GFP-tagged TOST-1, PICS-1, and ERH-2 and subjected the associated proteins to mass spectrometry (Figure S8; Table S1; summarized in Figure 6E). Combining both the *in vitro* and *in vivo* binding data, we conclude that TOFU-6, PICS-1, ERH-2, PID-1, and TOST-1 can form protein complexes in *C. elegans*.

Identification of IFE-3 as an Additional Factor Required for TOFU-6 Binding

To further understand the mechanism by which the PICS complex mediates 21U-RNA maturation, we identified IFE-3 from IP-MS assays of TOFU-6, PICS-1, TOST-1, and ERH-2

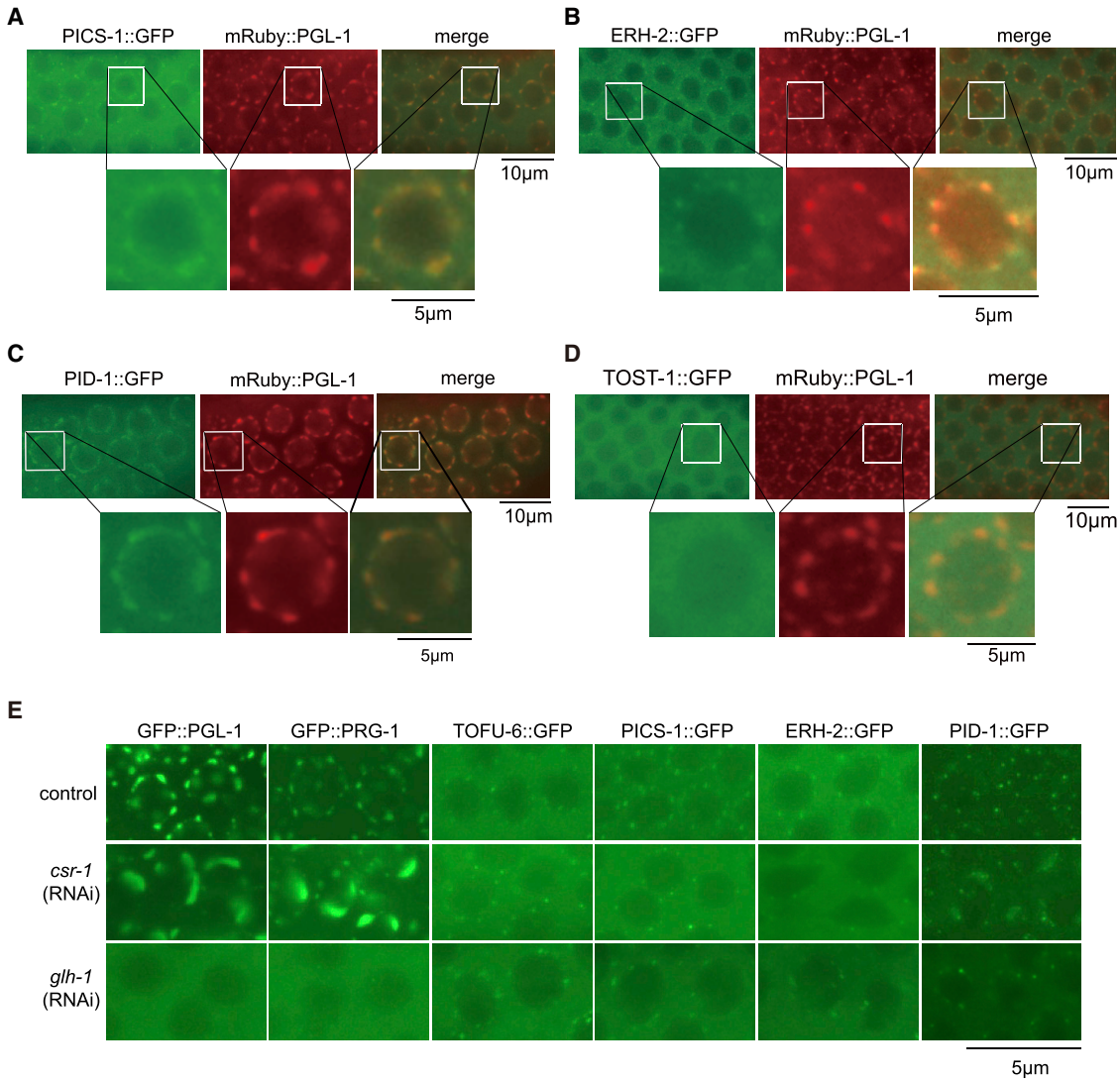

Figure 5. Subcellular Localization of PICS-1, ERH-2, PID-1, and TOST-1

(A–D) Images of PICS-1::GFP (A), ERH-2::GFP (B), PID-1::GFP (C), TOST-1::GFP (D), and the P-granule marker mRuby::PGL-1 in germ cells.

(E) Images of adult germline cells expressing indicated transgenes after feeding RNAi targeting *csr-1* and *glh-1*.

(Figure S8; Table S1). IFE-3 encodes one of the five *C. elegans* homologs of the mRNA cap-binding protein eIF4E, which is therefore predicted to bind capped RNAs and likely 21U-RNA precursors (Mangio et al., 2015). An *in vitro* GST pull-down assay further confirmed a direct protein-protein interaction between TOFU-6 and IFE-3 (Figure S9A).

Like *tofu-6*(*ust94*) mutants, *ife-3*(*tm6709*) animals were sterile (Figures S9B and S9C). However, although *tofu-6* mutants exhibited embryos inside gravid adults, *ife-3* animals contained no embryos inside at all, suggesting that IFE-3 and TOFU-6 may perform different roles during embryogenesis. We inserted a GFP tag at the C terminus of the IFE-3 coding sequence *in situ* with CRISPR/Cas9 technology. The IFE-3::GFP animals had brood sizes similar to those of wild-type animals, suggesting that the IFE-3::GFP transgene could recapitulate the functions of endogenous IFE-3 proteins (Figure S9C). IFE-3 largely co-localized with the P-granule marker PGL-1 in the germline as well (Figure S9D). However, depletion of *ife-3* did not change the perinuclear localization of TOFU-6, PICS-1, ERH-2, PID-1, or TOST-1 in germlines and embryos, respectively, and vice versa (data not shown).

TOFU-6, PICS-1, ERH-2, and TOST-1 Promote Chromosome Segregation and Cell Division

We tested whether PID-1, PICS-1, ERH-2, and TOST-1 are required for chromosome segregation and cell division, similar to TOFU-6. Using a GFP::H2B transgene, we found that TOFU-6, PICS-1, ERH-2, and TOST-1, but not PRG-1 and PID-1, are required for chromosome segregation and cell division in early embryos (Figures 7A and 7B), but not in the mitotic

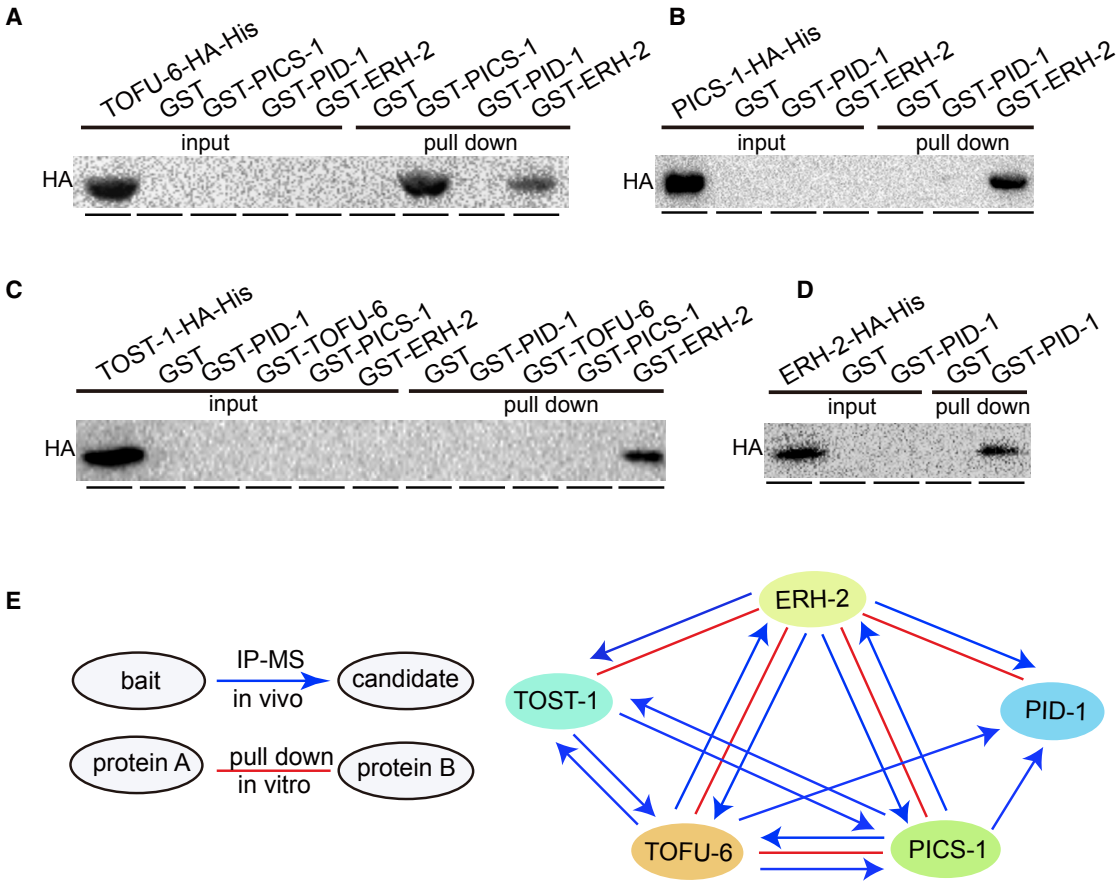

Figure 6. TOFU-6, PICS-1, ERH-2, PID-1, and TOST-1 Interact with Each Other Both *In Vitro* and *In Vivo*

(A–D) Western blotting of pull-down samples to assay protein-protein interactions among TOFU-6 (A), PICS-1 (B), TOST-1 (C), and ERH-2 (D) *in vitro*.

(E) Summary of the protein-protein interactions of TOFU-6, PICS-1, ERH-2, PID-1, and TOST-1 both *in vitro* and *in vivo*. Red lines indicate interactions *in vitro*. Blue arrows indicate interactions *in vivo*.

region in the germline (Figure S10A). In the absence of *tofu-6*, *pics-1*, *erh-2*, and *tost-1*, but not *pid-1* and *prg-1*, we observed chromosome-lagging and cell-bridging phenotypes. Since PRG-1 and PID-1 are both essential for 21U-RNA production, these results suggest that TOFU-6-, PICS-1-, and ERH-2-involved chromosome segregation and cell division processes are independent of 21U-RNA generation. Consistently, although *pid-1* and *prg-1* mutants had viable progeny, *tofu-6*, *pics-1*, *erh-2*, *and tost-1* mutants were sterile (Figures 1D and S6A). Unlike TOFU-6, PICS-1, ERH-2, and TOST-1, in the oocytes and embryos, PRG-1 only exhibits foci formation, and the expression of PID-1 is much weaker than its expression in the germline (Figures S1B and S6D).

We investigated the subcellular localization of TOFU-6, PICS-1, ERH-2, and TOST-1 in embryos. During early embryogenesis, TOFU-6, PICS-1, ERH-2, and TOST-1 entered the nucleus at the prophase of cell division, but remained in the cytosol at interphase without focus formation, in 2- and 4-cell embryos (Figures 7C and S10B). The subcellular localization of PICS factors exhibited mutual dependency (Figures 7D and S10C; summarized in Figure 7E).

Dual Roles of TOFU-6 in Promoting 21U-RNA Biogenesis and Chromosome Segregation

To further demonstrate that TOFU-6-, PICS-1-, and ERH-2-involved chromosome segregation and cell division processes are independent of 21U-RNA generation, we investigated the role of *tofu-6*(*ust95*) protein in mediating these two processes. Both *tofu-6*(*ust94*) and *tofu-6*(*ust95*) mutants were defective in 21U-RNA accumulation, but the *tofu-6*(*ust94*) was sterile while the *tofu-6*(*ust95*) was fertile (Figures 1C and 1D). Introduction of the GFP::TOFU-6(ust95) transgene can rescue the brood size of *tofu-6*(*ust94*) animals (Figure S11A). Although GFP::TOFU-6(ust95) could accumulate in the nucleus in early embryos as full-length TOFU-6 did, it failed to accumulate in perinuclear foci (Figures S11B and S11C), suggesting that the role of TOFU-6 to mediate chromosome segregation and cell division processes is independent of 21U-RNA biogenesis.

Then, we investigated whether TOFU-6(ust95) can bind to other PICS factors, similarly to full-length TOFU-6. Unfortunately, bacterially expressed HA (hemagglutinin)-His-tagged TOFU-6(ust95) formed insoluble aggregates during protein purification (data not shown). However, the N-terminal TOFU-6 RRM

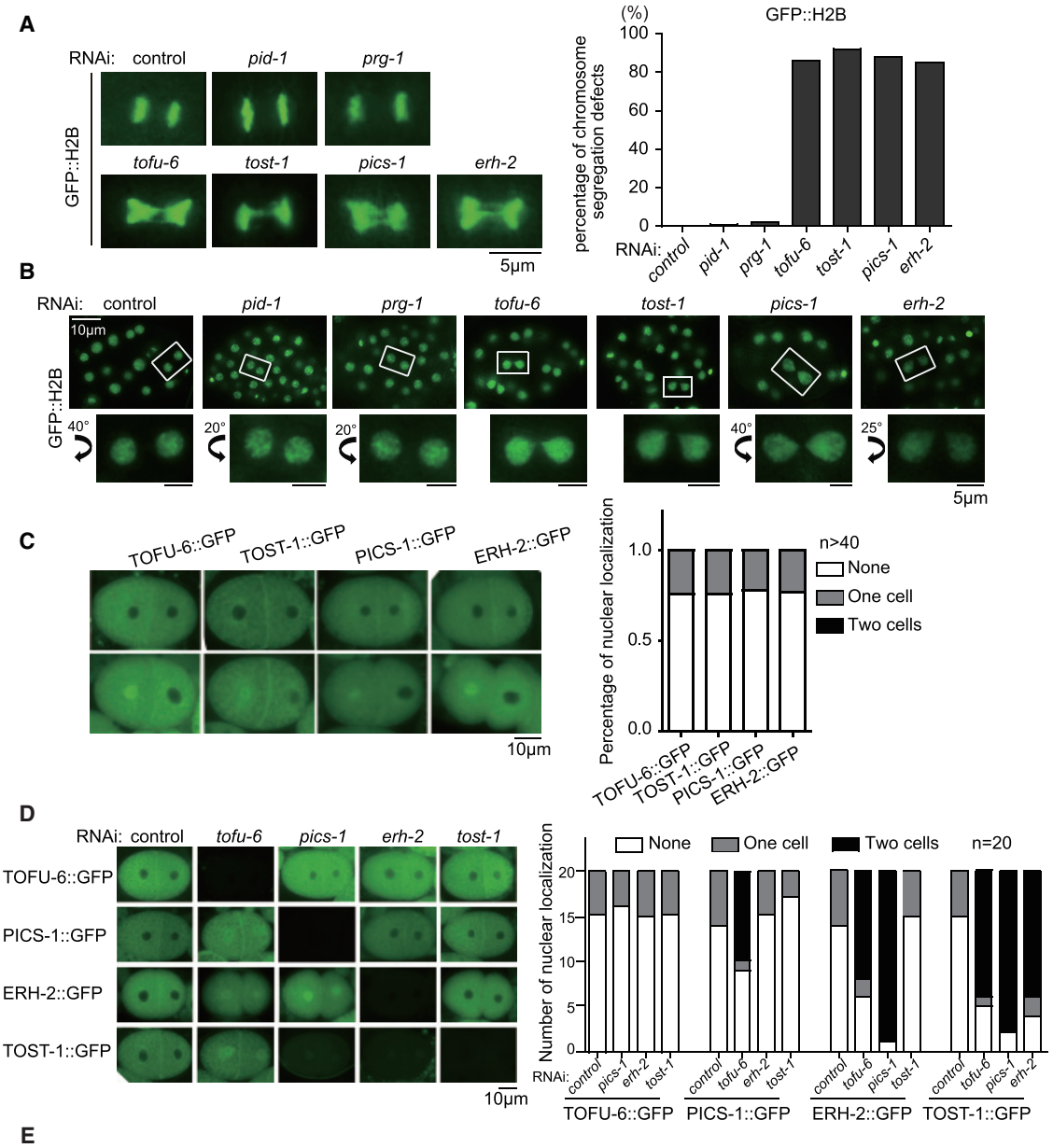

E

RNAi	control	*tofu-6*	*pics-1*	*erh-2*	*tost-1*
TOFU-6::GFP	cyt.	---	cyt.	cyt.	cyt.
PICS-1::GFP	cyt.	nuc.	---	cyt.	cyt.
ERH-2::GFP	cyt.	nuc.	nuc.	---	cyt.
TOST-1::GFP	cyt.	nuc.	nuc.	nuc.	---

Figure 7. TOFU-6, PICS-1, ERH-2, and TOST-1 Are Required for Chromosome Segregation and Cell Division

(A) Images of GFP::H2B at the meta-anaphase stage after RNAi targeting of the indicated genes in embryos (left). Diagram displaying the percentage of abnormal chromosome segregation (right).

(B) Images of GFP::H2B in late embryos after RNAi targeting of the indicated genes.

(C) Images of TOFU-6/PICS-1/ERH-2/TOST-1::GFP in two-cell embryos (left). Diagram displaying the percentage of TOFU-6/PICS-1/ERH-2/TOST-1::GFP accumulation in the nucleus in two-cell embryos (right).

(legend continued on next page)

domain was soluble. We purified the HA-His-tagged TOFU-6(RRM) domain from *E. coli* and found that it bound to PICS-1 and ERH-2, but not to PID-1 and TOST-1 (Figure S11D). Interestingly, the C-terminal domain of TOFU-6, a 298- to 345-amino-acid sequence, bound to IFE-3 but not to PICS-1 and ERH-2 (Figures S11E and S11F), suggesting that TOFU-6 uses distinct domains to associate with different co-factors.

DISCUSSION

Here, through a series of proteomics and imaging experiments, we demonstrate that in the germline, four proteins (TOFU-6, PICS-1, ERH-2, and PID-1) might function as a complex and promote the maturation of 21U-RNAs (Figure S12). In embryos, TOFU-6, PICS-1, ERH-2, and TOST-1 might form another complex and accumulate in the nucleus to engage in chromosome segregation and cell division. These factors exhibit dynamic localization among different subcellular compartments at different developmental stages. We speculate that differential compositions of these PICS factors may help cells coordinate distinct cellular processes.

TOFU-6, PICS-1, and ERH-2 Are Required for 21U-RNA Biogenesis

Previously, forward genetic screens have identified PRDE-1 and PID-1 as essential factors for 21U-RNA biogenesis in *C. elegans* (de Albuquerque et al., 2014; Weick and Miska, 2014). A genome-wide RNAi screening identified TOFU genes that are engaged in expression and distinct processing steps of 21U-RNAs (Goh et al., 2014). We recently found that TOFU-4/5, PRDE-1, and SNPC-4 form a USTC complex that associates with the upstream sequence element to promote the transcription of 21U-RNA precursors (Weng et al., 2019). Here, we combined a series of functional proteomic methods and identified a PICS complex containing TOFU-6, PICS-1, ERH-2, and PID-1 in the germline. We further used cell biology approaches and demonstrated mutual dependency of the components of the PICS complex in forming perinuclear granules. Using deep-sequencing technology, we found that 21U-RNA levels were reduced and precursors accumulated, which suggests that the TOFU-6, PICS-1, and ERH-2 proteins are engaged in 21U-RNA maturation.

The biochemical characteristics of the complex are unclear. In *tofu-6*, *pics-1*, and *erh-2* mutants, both capped and decapped 21U-RNA precursors accumulated, which suggests that the PICS factors act upstream PRG-1, binding to mature 21U-RNAs. IFE-3 directly binds to the C-terminal domain of TOFU-6, and IFE-3 binds to 5′-capped RNAs. It is possible that IFE-3 binds to capped 21U-RNA precursors; recruits TOFU-6, PID-1, PICS-1, and ERH-2; and initiates 5′-end decapping and trimming processes. Since we did not isolate decapping enzymes or exonucleases from the IP-MS experiments, further work is required to identify the actual enzyme and mechanisms of 21U-RNA maturation.

PARN-1 is a conserved exonuclease that is expressed in germline P-granules and is required for the 3′-end processing of 21U-RNAs (Tang et al., 2016). We did not identify PARN-1 from our IP-MS experiments, suggesting that PARN-1 and the PICS complex may act independently of each other to promote 21U-RNA maturation. For instance, the PICS complex may act to perform 5′ trimming of 21U-RNA precursors. Alternatively, their interaction may be too transient to be captured by IP-MS experiments.

TOFU-6, PICS-1, ERH-2, and TOST-1 Engage in Chromosome Segregation and Cell Division

Strikingly, we found that *tofu-6*, *pics-1*, *erh-2*, and *tost-1* mutants exhibited abnormal chromosome segregation and cell division during embryogenesis. These defects were independent of the presence of 21U-RNAs, since similar defects were not observed in *prg-1* and *pid-1* mutants. We speculate that TOFU-6, PICS-1, ERH-2, and TOST-1 may have direct roles in mediating chromosome segregation. In early embryos, TOFU-6, PICS-1, ERH-2, and TOST-1, but not PRG-1 and PID-1, could accumulate in the nucleus in mutually dependent manners.

The mechanism by which TOFU-6, PICS-1, ERH-2, and TOST-1 promote chromosome segregation is unclear. ERH, the human ortholog of ERH-2, has been shown to cooperate with conserved RNA-processing factors to promote meiotic mRNA decay and facultative heterochromatin assembly, affect the replication stress response through regulation of RNA processing, and control centromere protein E (CENP-E) mRNA splicing (Kavanaugh et al., 2015; Sugiyama et al., 2016; Weng et al., 2012). Whether TOFU-6, PICS-1, and TOST-1 act through ERH-2 to engage in chromosome segregation requires further investigation. Notably, both TOFU-6 and PICS-1 have RNA binding domains. It will also be interesting to identify the RNAs that bind to the PICS complex.

Differential Compositions of TOFU-6, PICS-1, ERH-2, PID-1, and TOST-1 in Distinct Subcellular Compartments

Cells organize many of their biochemical reactions in distinct subcellular compartments in which proteins and nucleic acids are concentrated. These subcellular compartments are involved in diverse processes, including RNA metabolism, ribosome biogenesis, DNA damage response, and signal transduction (Van Treeck and Parker, 2018). We show here that certain 21U-RNA processing factors, including TOFU-6, PICS-1, and ERH-2, localize to the perinuclear condensates, which we named PICS granules. We found that these factors were distributed in the cytoplasm, the perinuclear nuage, and the nucleus in mutually dependent manners. Moreover, the PICS granules exhibited a spatiotemporal distribution at distinct developmental

(D) Images of TOFU-6/PICS-1/ERH-2/TOST-1::GFP in two-cell embryos after RNAi targeting of the indicated genes (left). Diagram displaying the percentage of TOFU-6/PICS-1/ERH-2/TOST-1::GFP accumulation in the nucleus after RNAi targeting of the indicated genes (right).
(E) Summary of the subcellular localization of the indicated transgenes in embryos after feeding RNAi targeting of the indicated genes. cyt., cytoplasm; nuc., nucleus.

stages. While they assembled as perinuclear nuages in the adult germline, they disassembled in oocytes and early embryos. We speculate that differential compositions of the PICS complex in distinct subcellular compartments help to organize and coordinate different cellular processes, including 21U-RNA biogenesis, chromosome segregation, and cell division. With emerging high-resolution imaging technologies, it will be informative to further elucidate the compositions, dynamics, and biological roles of these PICS granules.

STAR★METHODS

Detailed methods are provided in the online version of this paper and include the following:

- KEY RESOURCES TABLE
- CONTACT FOR REAGENT AND RESOURCE SHARING
- EXPERIMENTAL MODEL AND SUBJECT DETAILS
  - *C. elegans* strains
- METHOD DETAILS
  - Construction of transgenic mutant strains
  - Immunoprecipitation followed by mass spectrometry analysis
  - RNAi
  - Microscope and images
  - RT-qPCR
  - RNA isolation and sequencing
  - Brood size
  - Protein expression and purification
  - GST pull-down
  - Western blotting
- QUANTIFICATION AND STATISTICAL ANALYSIS
  - RNA-seq analysis
  - Statistics
- DATA AND SOFTWARE AVALABILITY

SUPPLEMENTAL INFORMATION

Supplemental Information can be found online at https://doi.org/10.1016/j.celrep.2019.05.076.

ACKNOWLEDGMENTS

We are grateful to Dr. Guangshuo Ou's lab for the technical support and suggestions and to the members of the Guang lab for their comments. We are grateful to the International *C. elegans* Gene Knockout Consortium and the National Bioresource Project for providing the strains. Some strains were provided by the CGC, which is funded by the NIH Office of Research Infrastructure Programs (P40 OD010440). This work was supported by grants from the National Key R&D Program of China (2018YFC1004500 and 2017YFA0102900), the National Natural Science Foundation of China (31671346, 91640110, 31870812, and 31871300), the Major/Innovative Program of Development Foundation of Hefei Center for Physical Science and Technology (2017FXZY005), and the CAS Interdisciplinary Innovation Team.

AUTHOR CONTRIBUTIONS

C.Z. and S.G. designed the project; C.Z., C.W., X.W., Y.-H.Y., W.-J.L., D.X, M.H., S.L. and X.F. performed research; C.Z., C.W., X.W., and Y.-H.Y. contributed new reagents and analytic tools; C.Z. and C.W. analyzed data; C.Z. and S.G. wrote the paper.

DECLARATION OF INTERESTS

The authors declare no competing interests.

Received: December 3, 2018
Revised: April 8, 2019
Accepted: May 20, 2019
Published: June 18, 2019

REFERENCES

Ashe, A., Sapetschnig, A., Weick, E.M., Mitchell, J., Bagijn, M.P., Cording, A.C., Doebley, A.L., Goldstein, L.D., Lehrbach, N.J., Le Pen, J., et al. (2012). piRNAs can trigger a multigenerational epigenetic memory in the germline of C. elegans. Cell *150*, 88–99.

Bagijn, M.P., Goldstein, L.D., Sapetschnig, A., Weick, E.M., Bouasker, S., Lehrbach, N.J., Simard, M.J., and Miska, E.A. (2012). Function, targets, and evolution of Caenorhabditis elegans piRNAs. Science *337*, 574–578.

Batista, P.J., Ruby, J.G., Claycomb, J.M., Chiang, R., Fahlgren, N., Kasschau, K.D., Chaves, D.A., Gu, W., Vasale, J.J., Duan, S., et al. (2008). PRG-1 and 21U-RNAs interact to form the piRNA complex required for fertility in C. elegans. Mol. Cell *31*, 67–78.

Billi, A.C., Alessi, A.F., Khivansara, V., Han, T., Freeberg, M., Mitani, S., and Kim, J.K. (2012). The Caenorhabditis elegans HEN1 ortholog, HENN-1, methylates and stabilizes select subclasses of germline small RNAs. PLoS Genet. *8*, e1002617.

Chen, X., Xu, F., Zhu, C., Ji, J., Zhou, X., Feng, X., and Guang, S. (2014). Dual sgRNA-directed gene knockout using CRISPR/Cas9 technology in Caenorhabditis elegans. Sci. Rep. *4*, 7581.

Das, P.P., Bagijn, M.P., Goldstein, L.D., Woolford, J.R., Lehrbach, N.J., Sapetschnig, A., Buhecha, H.R., Gilchrist, M.J., Howe, K.L., Stark, R., et al. (2008). Piwi and piRNAs act upstream of an endogenous siRNA pathway to suppress Tc3 transposon mobility in the Caenorhabditis elegans germline. Mol. Cell *31*, 79–90.

de Albuquerque, B.F., Luteijn, M.J., Cordeiro Rodrigues, R.J., van Bergeijk, P., Waaijers, S., Kaaij, L.J., Klein, H., Boxem, M., and Ketting, R.F. (2014). PID-1 is a novel factor that operates during 21U-RNA biogenesis in Caenorhabditis elegans. Genes Dev. *28*, 683–688.

Feng, X., and Guang, S. (2013). Small RNAs, RNAi and the inheritance of gene silencing in Caenorhabditis elegans. J. Genet. Genomics *40*, 153–160.

Feng, G., Zhu, Z., Li, W.J., Lin, Q., Chai, Y., Dong, M.Q., and Ou, G. (2017). Hippo kinases maintain polarity during directional cell migration in Caenorhabditis elegans. EMBO J. *36*, 334–345.

Frøkjaer-Jensen, C., Davis, M.W., Hopkins, C.E., Newman, B.J., Thummel, J.M., Olesen, S.P., Grunnet, M., and Jorgensen, E.M. (2008). Single-copy insertion of transgenes in Caenorhabditis elegans. Nat. Genet. *40*, 1375–1383.

Goh, W.S., Seah, J.W., Harrison, E.J., Chen, C., Hammell, C.M., and Hannon, G.J. (2014). A genome-wide RNAi screen identifies factors required for distinct stages of C. elegans piRNA biogenesis. Genes Dev. *28*, 797–807.

Gu, W., Lee, H.C., Chaves, D., Youngman, E.M., Pazour, G.J., Conte, D., Jr., and Mello, C.C. (2012). CapSeq and CIP-TAP identify Pol II start sites and reveal capped small RNAs as C. elegans piRNA precursors. Cell *151*, 1488–1500.

Kavanaugh, G., Zhao, R., Guo, Y., Mohni, K.N., Glick, G., Lacy, M.E., Hutson, M.S., Ascano, M., and Cortez, D. (2015). Enhancer of Rudimentary Homolog Affects the Replication Stress Response through Regulation of RNA Processing. Mol. Cell. Biol. *35*, 2979–2990.

Kim, K.W., Tang, N.H., Andrusiak, M.G., Wu, Z., Chisholm, A.D., and Jin, Y. (2018). A Neuronal piRNA Pathway Inhibits Axon Regeneration in C. elegans. Neuron *97*, 511–519 e516.

Langmead, B., and Salzberg, S.L. (2012). Fast gapped-read alignment with Bowtie 2. Nat. Methods *9*, 357–359.

Lee, H.C., Gu, W., Shirayama, M., Youngman, E., Conte, D., Jr., and Mello, C.C. (2012). C. elegans piRNAs mediate the genome-wide surveillance of germline transcripts. Cell *150*, 78–87.

Li, H., Handsaker, B., Wysoker, A., Fennell, T., Ruan, J., Homer, N., Marth, G., Abecasis, G., and Durbin, R.; 1000 Genome Project Data Processing Subgroup (2009). The Sequence Alignment/Map format and SAMtools. Bioinformatics *25*, 2078–2079.

Luteijn, M.J., and Ketting, R.F. (2013). PIWI-interacting RNAs: from generation to transgenerational epigenetics. Nat. Rev. Genet. *14*, 523–534.

Malone, C.D., and Hannon, G.J. (2009). Molecular evolution of piRNA and transposon control pathways in Drosophila. Cold Spring Harb. Symp. Quant. Biol. *74*, 225–234.

Mangio, R.S., Votra, S., and Pruyne, D. (2015). The canonical eIF4E isoform of C. elegans regulates growth, embryogenesis, and germline sex-determination. Biol. Open *4*, 843–851.

Mao, H., Zhu, C., Zong, D., Weng, C., Yang, X., Huang, H., Liu, D., Feng, X., and Guang, S. (2015). The Nrde Pathway Mediates Small-RNA-Directed Histone H3 Lysine 27 Trimethylation in Caenorhabditis elegans. Curr. Biol. *25*, 2398–2403.

Minasaki, R., and Streit, A. (2007). MEL-47, a novel protein required for early cell divisions in the nematode Caenorhabditis elegans. Mol. Genet. Genomics *277*, 315–328.

Rodrigues, R., Domingues, A., Hellmann, S., Dietz, S., de Albuquerque, B., Renz, C., Ulrich, H.D., Butter, F., and Ketting, R. (2018). PETISCO is a novel protein complex required for 21U RNA biogenesis and embryonic viability. bioRxiv. https://doi.org/10.1101/463711.

Ruby, J.G., Jan, C., Player, C., Axtell, M.J., Lee, W., Nusbaum, C., Ge, H., and Bartel, D.P. (2006). Large-scale sequencing reveals 21U-RNAs and additional microRNAs and endogenous siRNAs in C. elegans. Cell *127*, 1193–1207.

Schneider, C.A., Rasband, W.S., and Eliceiri, K.W. (2012). NIH Image to ImageJ: 25 years of image analysis. Nat. Methods *9*, 671–675.

Shen, E.Z., Chen, H., Ozturk, A.R., Tu, S., Shirayama, M., Tang, W., Ding, Y.H., Dai, S.Y., Weng, Z., and Mello, C.C. (2018). Identification of piRNA Binding Sites Reveals the Argonaute Regulatory Landscape of the C. elegans Germline. Cell *172*, 937–951 e918.

Shirayama, M., Seth, M., Lee, H.C., Gu, W., Ishidate, T., Conte, D., Jr., and Mello, C.C. (2012). piRNAs initiate an epigenetic memory of nonself RNA in the C. elegans germline. Cell *150*, 65–77.

Sugiyama, T., Thillainadesan, G., Chalamcharla, V.R., Meng, Z., Balachandran, V., Dhakshnamoorthy, J., Zhou, M., and Grewal, S.I.S. (2016). Enhancer of Rudimentary Cooperates with Conserved RNA-Processing Factors to Promote Meiotic mRNA Decay and Facultative Heterochromatin Assembly. Mol. Cell *61*, 747–759.

Tang, W., Tu, S., Lee, H.C., Weng, Z., and Mello, C.C. (2016). The RNase PARN-1 Trims piRNA 3′ Ends to Promote Transcriptome Surveillance in C. elegans. Cell *164*, 974–984.

Timmons, L., Court, D.L., and Fire, A. (2001). Ingestion of bacterially expressed dsRNAs can produce specific and potent genetic interference in Caenorhabditis elegans. Gene *263*, 103–112.

Van Treeck, B., and Parker, R. (2018). Emerging Roles for Intermolecular RNA-RNA Interactions in RNP Assemblies. Cell *174*, 791–802.

Watanabe, T., and Lin, H. (2014). Posttranscriptional regulation of gene expression by Piwi proteins and piRNAs. Mol. Cell *56*, 18–27.

Weick, E.M., and Miska, E.A. (2014). piRNAs: from biogenesis to function. Development *141*, 3458–3471.

Weick, E.M., Sarkies, P., Silva, N., Chen, R.A., Moss, S.M., Cording, A.C., Ahringer, J., Martinez-Perez, E., and Miska, E.A. (2014). PRDE-1 is a nuclear factor essential for the biogenesis of Ruby motif-dependent piRNAs in C. elegans. Genes Dev. *28*, 783–796.

Weng, M.T., Lee, J.H., Wei, S.C., Li, Q., Shahamatdar, S., Hsu, D., Schetter, A.J., Swatkoski, S., Mannan, P., Garfield, S., et al. (2012). Evolutionarily conserved protein ERH controls CENP-E mRNA splicing and is required for the survival of KRAS mutant cancer cells. Proc. Natl. Acad. Sci. USA *109*, E3659–E3667.

Weng, C., Kosalka, J., Berkyurek, A.C., Stempor, P., Feng, X., Mao, H., Zeng, C., Li, W.J., Yan, Y.H., Dong, M.Q., et al. (2019). The USTC co-opts an ancient machinery to drive piRNA transcription in *C. elegans*. Genes Dev. *33*, 90–102.

Zhang, D., Tu, S., Stubna, M., Wu, W.S., Huang, W.C., Weng, Z., and Lee, H.C. (2018). The piRNA targeting rules and the resistance to piRNA silencing in endogenous genes. Science *359*, 587–592.

STAR★METHODS

KEY RESOURCES TABLE

REAGENT or RESOURCE	SOURCE	IDENTIFIER
Antibodies		
Anti-GFP antibody	Abcam	Cat#ab290; RRID: AB_303395
Anti-β-actin	Servicebio	Cat#GB12001
Anti-HA	Proteintech	Cat#66006-1-Ig;
Anti-Mouse IgG(H+L)	proteintech	Cat#SA00001-1; RRID: AB_2722565
Bacterial and Virus Strains		
N/A	N/A	N/A
Biological Samples		
N/A	N/A	N/A
Chemicals, Peptides, and Recombinant Proteins		
CIAP	Invitrogen	Cat#18009019
Tabacco decapping plus 2 (TDP2)	Enzymax	Cat#94
DNase I	Thermo Fisher	Cat#18047019
Critical Commercial Assays		
GoScript Reverse Transcription System	Promega	Cat#A5000/A50001
SYBR Green	Vazyme	Cat#Q111-02/03
ClonExpress MultiS One Step Cloning Kit	Vazyme	Cat#C113-02
Deposited Data		
RNaseq data	This Paper	GEO: GSE130317
Experimental Models: Cell Lines		
N/A	N/A	N/A
Experimental Models: Organisms/Strains		
C. elegans Strains, see Table S2	This Paper	N/A
Oligonucleotides		
Primers for transgenes construction and sgRNA-mediated gene editing, see Table S3	This Paper	N/A
Primers for RT and qRT assays, see Table S4	This Paper	N/A
Recombinant DNA		
N/A	N/A	N/A
Software and Algorithms		
ImageJ	(Schneider et al., 2012)	https://imagej.nih.gov/ij/
Bowtie2	(Langmead and Salzberg, 2012)	N/A
Samtools	(Li et al., 2009)	N/A
Other		
N/A	N/A	N/A

CONTACT FOR REAGENT AND RESOURCE SHARING

Further information and requests for resources and reagents should be directed to and will be fulfilled by the Lead Contact, Shouhong Guang (sguang@ustc.edu.cn).

EXPERIMENTAL MODEL AND SUBJECT DETAILS

C. elegans strains

The Bistol strain N2 was used as the standard wild-type strain. All strains were grown at 20°C unless other specified. The strains used in this study are listed in Table S2. To collect homozygous mutant worms, the balanced worms were synchronized and about 1000 homozygous mutants were collected when they reached the late young adult stage.

METHOD DETAILS

Construction of transgenic mutant strains

For TOFU-1::GFP, TOFU-2::GFP, TOFU-6::GFP, PID-1::GFP, PICS-1::GFP, TOST-1::GFP, and TOFU-6(ust95)::GFP endogenous promoter sequences, 3′ UTR, ORFs, coding sequence for gfp::3xflag and a linker sequence (GGAGGTGGAGGTGGAGCT) (inserted between the ORFs and gfp::3xflag) were fused and cloned into PCFJ151 vectors using a ClonExpress MultiS One Step Cloning Kit (Vazyme C113-02, Nanjing). These transgenes were integrated into the *C. elegans'* chromosome II by MosSCI technology.

For ERH-2::GFP, IFE-3::GFP and GFP::PRG-1, the coding sequence of gfp::3xflag was inserted before the stop codon or after the initiation codon using the CRISPR-Cas9 system. The repair templates contained homologous arms of 1000 bp to 1500 bp and were cloned into a vector using the ClonExpress MultiS One Step Cloning Kit. The injection mix contained PDD162 (50 ng/μL), a repair plasmid (50 ng/μL), pcfj90 or 90-gfp (20 ng/μL) and one or two gRNAs close to the N-terminals or C-terminals of the genes (20 ng/μL). The mix was injected into young adult N2 animals. Two or three days later, F1 worms containing the pcfj90 or 90-gfp marker were isolated. After growing at 20°C for another three days, the animals were screened for GFP insertion by PCR.

For gene deletions, 3 or 4 sgRNAs were coinjected into N2, +/mIn1 or +/qC1 animals with PDD162 (50 ng/μL), pcfj90 (20 ng/μL), 10xTE buffer, and DNA ladder (500 ng/μL). Two or three days later, F1 worms expressing the pcfj90 marker were isolated. After growing at 20°C for another three days, the animals were screened for deletions by PCR.

The primers used for molecular cloning and dual-sgRNA-directed CRISPR/Cas9-mediated gene deletion are listed in Table S3.

Immunoprecipitation followed by mass spectrometry analysis

Mix-stage transgenic worms expressing TOFU-6::GFP, TOST-1::GFP, PICS-1::GFP, and ERH-2::GFP were resuspended in equal volumes of 2x lysis buffer (50 mM Tris-HCl pH 8.0, 300 mM NaCl, 10% glycerol, 1% Triton X-100, Roche®cOmplete EDTA-free Protease Inhibitor Cocktail, 10 mM NaF, and 2 mM Na_3VO_4) and lysed in a FastPrep-24 5G homogenizer. The supernatant of the lysate was incubated with homemade anti-GFP beads for one hour at 4°C. The beads were then washed three times with cold lysis buffer. The GFP immunoprecipitates were eluted with chilled elution buffer (100 mM glycine-HCl pH 2.5). Approximately 1/8 of the eluates were subjected to western blotting analysis. The rest of the eluates were precipitated with TCA or cold acetone and dissolved in 100 mM Tris, pH 8.5, with 8 M urea. The proteins were reduced with TCEP, alkylated with IAA, and finally digested with trypsin at 37°C overnight. LC-MS/MS analysis of the resulting peptides and MS data processing approaches were conducted as previously described (Feng et al., 2017). A WD scoring metrix was used to identify high-confidence candidate interacting proteins.

RNAi

RNAi experiments were conducted as previously described (Timmons et al., 2001).

Microscope and images

Images were collected on Leica DM2500 microscope. For the quantitation of GFP intensity, the average fluorescence intensities of adult worms (0.5 s exposure) were analyzed using ImageJ. For stitched images, individual images were collected by shifting the slides horizontally and then were stitched manually in overlapped regions.

RT-qPCR

RNA was isolated from the indicated animals and subjected to DNase I digestion (Thermo Fisher). cDNA was generated from the RNA using a GoScript Reverse Transcription System (Promega) according to the vendor's protocol. qPCR was performed using a MyIQ2 real-time PCR system(Bio-Rad) with AceQ SYBR Green Master mix(Vazyme). The primers used in RT-qPCR are listed in Table S4. *Eft*-3 mRNA was used as an internal control for sample normalization.

RNA isolation and sequencing

Synchronized late young adult worms were sonicated in sonication buffer (20 mM Tris-HCl,pH 7.5, 200 mM NaCl, 2.5 mM $MgCl_2$, and 0.5% NP40). The eluates were incubated with TRIzol reagent and then precipitated with isopropanol. The precipitated RNA was treated with calf intestinal alkaline phosphatase (CIAP, Invitrogen), re-extracted with TRIzol, and treated with or without Tobacco Decapping Plus 2 (TDP2, Enzymax, cat. #94) before library construction.

Small RNAs were subjected to deep sequencing using an Illumina platform (Novogene Bioinformatics Technology Co., Ltd.). Briefly, small RNAs ranging from 18 to 30 nt were gel-purified and ligated to a 3′ adaptor (5′-pUCGUAUGCCGUCUUCUGCUUGidT-3′; p, phosphate; idT, inverted deoxythymidine) and a 5′ adaptor (5′-GUUCAGAGUUCUACAGUCCGACGAUC-3′). The ligation products

were gel-purified, reverse transcribed, and amplified using an Illumina sRNA primer set (5′-CAAGCAGAAGACGGCATACGA-3′; 5′-AAT GATACGGCGACCACCGA-3′). The samples were then sequenced using an Illumina HiSeq platform.

Brood size

L3 worms were placed individually into fresh NGM plates, and the progeny numbers were scored.

Protein expression and purification

GST-tagged proteins were cloned into the vector PGEX-4T-1, and HA-tagged proteins were cloned into the vector PET22b. All expression plasmids were transformed into *E. coli* Rosetta(DE3) and the proteins were expressed at 16°C for 20 hours in the presence of 0.5 mM IPTG. The recombinant proteins, which contained an N-terminal GST-tag, were purified on Glutathione Sepharose (GE Healthcare). The recombinant proteins, which contained a C-terminal HA-tag and a 6 × His tag, were purified on Ni-NTA resin (GE Healthcare).

GST pull-down

Recombinant GST-fused proteins were incubated with Glutathione Sepharose (GE Healthcare) in buffer (20 mM Tris, 200 mM NaCl, pH 7.5) for 40 min at 4°C. Then HA-tagged protein was added, and the mixture was incubated for 40 min at 4°C. The resin was then washed three times with buffer (20 mM Tris, 200 mM NaCl, pH 7.5, 2 mM DTT, 0.1% NP-40). Finally, 50 mM glutathione was added and incubated for 30 min to elute the protein. All GST pulldown samples were loaded onto a SDS-PAGE and then transferred to a Hybond-ECL membrane for western blotting.

Western blotting

Proteins were resolved by SDS-PAGE on gradient gels (10% separation gel, 5% spacer gel) and transferred to a Hybond-ECL membrane. After washing with TBST buffer (Sangon Biotech, Shanghai) and blocking with 5% milk-TBST, the membrane was incubated at room temperature for two hours with antibodies (listed below). After 3 × 10min washes in TBST, the membrane was incubated at room temperature for an additional two hours with secondary antibodies. The membrane was washed for 3 × 10min in TBST and then visualized. The antibody dilution for the western blots were as follows: GFP (Abcam ab290), 1:5000; β-actin (Servicebio GB12001), 1:2000; and His (Proteintech 66006-1-Ig), 1:5000. Anti-HA Ab and anti-mouse IgG (H+L) were purchased from Proteintech.

QUANTIFICATION AND STATISTICAL ANALYSIS

RNA-seq analysis

The Illumina-generated raw reads were first filtered to remove adaptors, low-quality tags and contaminants to obtain clean reads at Novogene. For mature piRNA analysis, clean reads ranging from 18 to 30 nt were mapped to the unmasked *C. elegans* genome and the transcriptome assembly WS243, respectively, using Bowtie2 with default parameters. For pre-piRNA analysis, the clean reads were mapped to known *C. elegans* 21U-RNA loci with 2 nt upstream and 3 nt downstream which included precursors and likely other intermediates and degradation products with 1 nt or 2 nt upstream and/or 1nt, 2nt or 3nt downstream, while the reads identical to mature 21U-RNA regions were excluded. The number of reads targeting each transcript was counted using custom Perl scripts.

Statistics

Bar graphs with error bars represented the mean and SD. All of the experiments were conducted with independent *C. elegans* animals for the indicated N replicates. Statistical analysis was performed with two-tailed Student's t tests or unpaired Wilcoxon tests. Student's t test p value threshold was set to 0.05.

DATA AND SOFTWARE AVALABILITY

All related data and materials are available upon request. The dataset of small RNA deep sequencing reported in this paper has been deposited in the Gene Expression Omnibus (GEO) database, https://www.ncbi.nlm.nih.gov/geo (accession number GEO: GSE130317).